Predicting performance of optical systems undergoing thermal/mechanical loadings using integrated thermal/structural/optical numerical methods

Jacob Miller
Marcus Hatch
Kenneth Green
Honeywell Inc.
Electro-Optics Center
2 Forbes Road
Lexington, Massachusetts 02173

Abstract. Predicting performance of electro-optical systems that operate while being subjected to thermal/mechanical loadings has been accomplished by integrating computer-based numerical tools. Honeywell has interfaced thermal, structural, and optical computer programs on both CDC 6600 and Honeywell 6080 computers into a Thermal/Structural/Optical (TSO) evaluation process. The TSO process integrates the separate analyses by automatizing data transfers among the individual technology programs to permit rapid evaluation of optical systems undergoing thermal/mechanical loadings.

The design/analysis process involves iterating the following: thermal/mechanical error budgets, TSO evaluations of electro-optical systems, and comparisons of TSO results with error budget line items. This paper presents how the TSO process has interfaced the individual technology programs, examples of TSO applications to Honeywell electro-optics systems, and test data from systems that have been subjected to thermal/mechanical loadings. The thermal/mechanical loadings include cryogenic loads, steady state acceleration, random vibration, and decaying dynamic loads.

The examples show how the process has been effectively used during the design/analysis stages of projects to evaluate alternate design concepts. The resulting process has resulted in a cost-effective methodology for predicting performance of electro-optical systems undergoing theral/mechanical loadings.

Keywords: optomechanical design; optical system performance predictions; numerical analysis methods.

Optical Engineering 20(2), 166-174 (March/April 1981).

CONTENTS

1. INTRODUCTION

Design and evaluation of electro-optical sensors that are undergoing thermal/mechanical loadings and resulting deformations require efficient computer analysis methods. Optical performance predictions should include predicted deformations caused by environmentally induced thermal/mechanical distortions in addition to fabrication tolerances and assembly strains. The thermal/mechanical distortions discussed in this paper can be caused by the following:

1. Thermal soaks of systems containing different materials;
2. Thermal gradients of systems having the same or different materials;
3. Spinning centrifugal, constant rotational velocity, loadings;
4. Mechanical shock specified as functions of time;
5. Mechanical shock specified as functions of spectra;
6. Sinusoidal vibration; and
7. Random vibration.

The integrated design/analysis cycles begin with defining requirements for thermal/structural performance based on electro-optical system requirements. These system requirements are then transformed into deformation and stress criteria for the thermal/structural design. These criteria are typically composed of the relevant material yield and microyield stress criteria and mechanical stability error budgets (after fabrication and assembly). The overall allocation in mechanical stability error budgets is obtained from electro-optical system error budgets to account for errors such as line-of-sight shifts, figure quality, 90% (or other criteria) of energy within given wavelengths to be within a particular area; surface deformations; de-focus. Optical sensitivities are initially used to allocate thermal/structural deformations (tilts, de-centers, axial despacing, surface deformations) among the possible deformation of all electro-optical components.

Subsequent to predictions of actual electro-optical system performance under thermal/mechanical loadings, the predicted thermal/structural deformations are compared to error budget line items. If predictions exceed error budget line items, re-allocations of error budget line items are made while maintaining the overall error budget allocations from system budgets. However, if reallocation of error budget line items will still not meet the overall error budget, then design/analysis cycle(s) with re-design, error

Invited paper OM-103 received Sep. 30, 1980; revised manuscript received and accepted for publication Oct. 27, 1980. This paper is a revision of Paper 216-21 which was presented at the SPIE seminar on Optics in Adverse Environments, Feb 4-5, 1980, Los Angeles, CA. The paper presented there appears (unrefereed) in SPIE Proceedings Vol. 216.

budget line item allocation, and analysis with comparisons to error budget line items will be necessary in order to meet electro-optical system requirements.

Evaluation of infrared cryogenic sensors undergoing thermal/mechanical loadings and subsequent distortions require efficient computer analysis methods. The design and evaluation process has been addressed at Honeywell by developing automatic data transfer computer codes that interface separate general purpose thermal, structural, and optical computer programs. This computer-aided design process[1] is referred to as our unique Thermal/Structural/Optical (TSO) integrated design analysis process.

The TSO process includes thermal, structural, and optical analyses. Although the individual thermal, structural, and optical analyses are not new, the interfacing of these analyses is new in the optical industry. The interfacing of these analyses is an important tool in performing cost-effective system analysis that often requires several design/analysis iterations. Interfacing of the separate analyses for the purpose of data transfer had been performed at Honeywell by outputs of each analyses being transformed and cardpunched into the next analysis. This technique was often a slow and costly process when design schedules could not tolerate time-consuming iterations. We have addressed this data transfer problem by writing interface codes and modifying existing computer programs in order to automate the data transfer among the separate analyses. TSO permits us to rapidly evaluate alternate designs and effects of design changes on optical performance of electro-optical sensors subjected to thermal and mechanical loads during transportation, nonoperational conditions, and operations when sensors are to meet system specs and requirements.

This paper presents results of design, analyses, and testing cycles of sensors for which the mechanical stability error budgeting and TSO processes have been applied. The process has been applied to various sensors containing metallic telescopes, re-imaging systems, interferometer, thermal imaging set, and detector/dewar assemblies. Description is given for the error budget process, TSO process and examples of the error budgeting and TSO process along with empirical data for several sensors. Data are also presented concerning cost savings and schedule reductions made possible with the methodology of evaluating sensors that are subjected to thermal/mechanical loadings. The following sections of this paper present discussions of the design/analysis techniques that include defining thermal/structural criteria and error budgets, TSO process, interactive thermal/structural modeling, and analyses along with examples (including empirical data)[2] of applications of the methodology to sensors.

2. THERMAL/STRUCTURAL CRITERIA AND ERROR BUDGETS

The design/analysis process to predict electro-optical system performance begins with defining thermal/structural criteria and mechanical stability error budgets. Although criteria and error budgeting are different among the various sensors, there is some level of commonality. Typically the thermal/structural criteria can be defined as follows:

- Temperatures of components may not exceed maximum allowable nonoperational and operational temperatures as determined from vendors' data and empirical data.
- Stresses, in electro-optical components and structural subsystems that are to maintain mechanical stability, shall be less than material microyield stresses with safety factor equal to

$$\frac{\text{Material Micro-Yield Stress}}{\text{Predicted Stress}} \geq 1.5 .$$

- Stresses, in components and structural subsystems that do not have to maintain mechanical stability, shall be less than material yield stresses with safety factor equal to

$$\frac{\text{Material Yield Stress}}{\text{Predicted Stress}} \geq 1.5 .$$

- Predicted deformations shall be less than the mechanical stability error budget line items.

The mechanical stability error budgets (herein referred to as the error budgets) use the values defined by system error budgets as the total allocation for each type of error. The types of errors, depending on system requirements, may be line-of-sight (LOS) shifts, figure quality, 90% (or other criteria) of energy to be within a particular area for given wavelengths, surface deformations, and defocus. The most typical are LOS shifts and figure quality changes versus system specs. Prior to design/analyses, initial budgeting is based on the overall allocation for each type of error (from system error budgets), electro-optical sensitivities, and performance experience with the type of system being designed. The result is an initial thermal/structural error budget that is expected to be close to, within minor perturbations, the final error budgets. The optical sensitivities used to initially allocate error budget line items are assumed to be linear over the expected range of surface deformation. Final optical system evaluation will predict the result of perturbing the optical design with thermal/structural deformations.

For each type of error, tabulations are made of thermal/structural deformation types, optical sensitivities, allocated error budget line items, and error contributions. Depending on the application and dynamic environments, the error budget line items are algebraically added, absolute value added, RSS'ed, or combinations of these, depending on how subsystems are expected to affect the error type. If the total effect of the allocated error budget line items exceeds the total allocated error, re-allocation is performed while maintaining the total error. These error budgets (all line items) are compared to predictions of environmentally induced thermal/structural deformations during design/analysis cycles. If predicted deformations exceed error budget line items, then re-allocation of line items (while maintaining total error allocation) is performed. If re-allocation will not meet total error allocation, then redesign/analyses cycles are performed.

3. THERMAL/STRUCTURAL/OPTICAL (TSO) PROCESS

The thermal/structural/optical (TSO) analysis flow shown in Fig. 1 interfaces on the CDC 6600 the following: MITAS (thermal

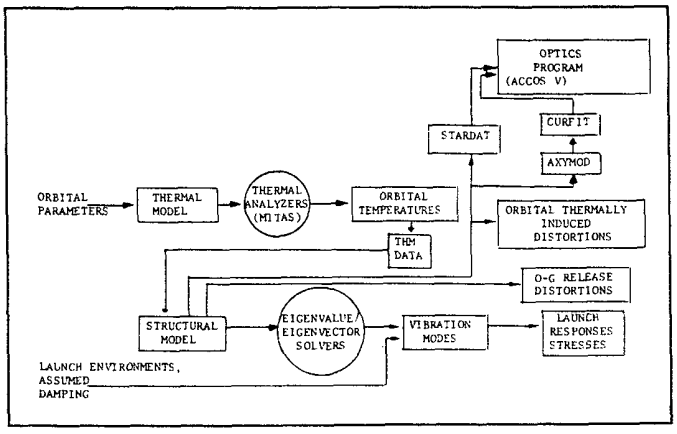

Fig. 1. Flow chart of thermal/structural/optical computer programs.

analysis code) to STARDYNE, AXY (structural analysis code) to ACCOS V (optical analysis). MITAS results are temperature maps that are interfaced with structural dynamics inputs into a structural model to predict deformation distributions that are interfaced with optical analysis programs that predict optical performance in-

cluding focal plane line-of-sight (LOS) shifts and blur circle size. (A similar program flow has been developed for the H6080 computer). In addition to reducing costs and task times, the interface codes perform nonlinear interpolation computations (not performed by nonautomatized data transfer) that increase accuracies of the analyses. The contribution to the state of the art includes both cost and time savings and improved accuracies in the automated data transfer process presented in this paper.

The analysis programs and interface codes are listed below:

3.a. Analysis programs

1. MITAS thermal program. General-purpose finite difference thermal analysis program.
2. AXY structural program. Finite element program for predicting deformations and stresses on rotationally symmetric structures subjected to acceleration, pressure and/or thermal environments.
3. STARDYNE structural program. General-purpose finite element structural analysis program for predicting natural vibration modes, static and dynamic deformations and stresses.
4. ACCOS V. General-purpose optical design, automatic optimization, and evaluation program. The types of evaluations include ray tracing, geometrical blur size, wave aberration variance, diffraction OTF and point spread function. The program can model a broad range of optical systems, such as zoom lenses, anamorphic lenses, tilted and decentered elements, conic surfaces, and nonrotationally symmetric surfaces.

3.b. Interface codes

1. THMDATA is an interface code to interface either the STARDYNE or AXYMOD structural analysis programs to the thermal analysis program MITAS. MITAS program is executed as if the restart option was being planned by saving TAPE22. The MITAS run will produce, in addition to printed thermal results, a tape (to be saved) having records (2) of temperature(s) labeled ST---- that may be processed by the T/S interface code THMDATA.

   THMDATA interface codes have two subprograms so that MITAS can be interfaced with either the structural analysis programs AXYMOD or STARDYNE. The two subprograms called THMAXY and THMSTAR interface MITAS to AXY and STARDYNE, respectively.
2. The THMDATA to STARDYNE data transfer is accomplished by adding nine job control language cards to the STARDYNE job control language deck.
3. STARDAT is an interface code to interface the structural analysis program STARDYNE with the ACCOS V optical analysis programs.

   STARDAT has two independent subprograms named TILTS and WAVES. TILTS is used for system evaluations of motion at each optical element's vertex for cases where optics can be modeled to move as rigid bodies. WAVES is used to evaluate the surface deformations of optical elements.
4. AXYMOD is a combined structural analysis program and interface code with ACCOS V. AXYMOD contains a finite element structural analysis program named AXY that is used to analyze rotationally symmetric structures subjected to concentrated forces, pressures, acceleration forces and/or thermal loads. The interface code portion of AXYMOD permits the user to define nodes corresponding to locations on subsequent optical analyses. AXYMOD prints the deformations, optical sags (motion of nodes in the direction parallel to optical axis) and fractional apertures (nodal radial position after deformation/undeformed optical element radius). The optical analysis program ACCOS V can use the AXYMOD output for performing optical analyses of optical elements undergoing (static) environmentally caused deformations.
5. CURFIT interfaces the structural analysis programs STARDAT and AXYMOD to the optical analysis program ACCOS V. CURFIT takes the changes in the surface nodal points and fits them to a nonrotationally symmetric polynomial. The deformed surface is defined by a table of optical sags which are calculated over a square grid of points covering the surface. The program generates punched output consisting of the optical sags and their (x,y) coordinates. These data are used directly by the ACCOS V spline function routine. An arbitrary point on the deformed surface is defined by interpolation between the closest known sags. The deformed sensor can now be evaluated using any criteria available to ACCOS V.

4. INTERACTIVE THERMAL/STRUCTURAL MODELING AND ANALYSES

The thermal and structural modeling and analysis portion of the TSO process uses well-known, established and universally used finite difference[3] thermal analysis programs (MITAS, SINDA) and finite element structural analysis programs (STARDYNE, ANSYS, AXY).[4] There will be no effort here to review how these individual programs perform thermal and structural analyses. These (individual) thermal analysis and structural analysis programs have been used at Honeywell to analyze sensors for thermal and structural effects prior to the TSO interfacing process. Papers have been published by various electro-optical design/analysis personnel giving thermal and structural predictions along with empirical data. Others have shown how structural deformations could be input to optics codes in order to assess effects of structural perturbations of optical performance. The results presented in the next section of this paper will be comparisons of predictions obtained with the automated TSO process to error budgets and to empirical data.

An extension of the TSO process, starting in 1979, has been to input thermal model data via time-share terminal and to perform interactive time-share structural modeling, model debugging, and structural analyses via the CDC UNISTRUC code.[5] UNISTRUC (see Fig. 2) permits the structural analyst to perform structural

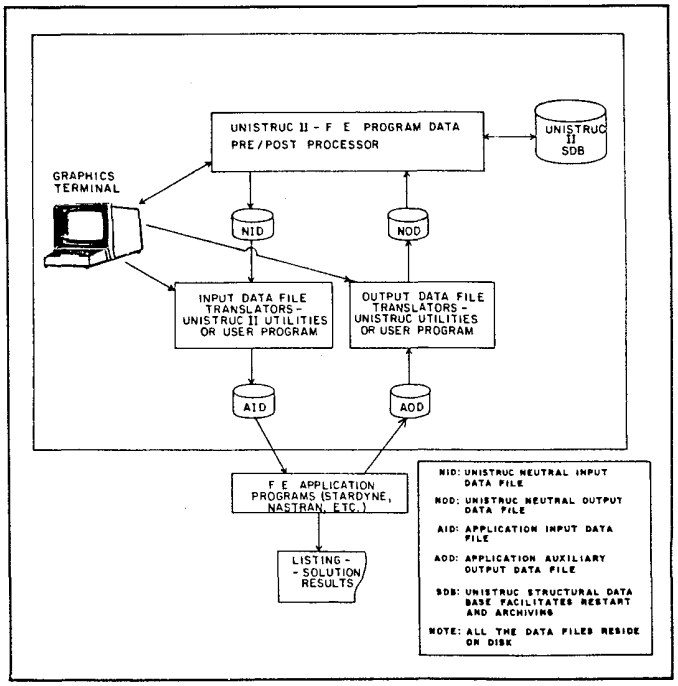

Fig. 2. UNISTRUC II—finite element application program interface environment.

modeling by having data input with either keyboard into a

Tektronix 4014 or by following lines on a drawing with a pressure sensitive pen on a digitizing tablet that is connected to a Tektronix 4014. UNISTRUC displays the model on a storage tube (part of the Tektronix 4014), and this permits the analyst to perform and modify debugging, rotation, zoom, and other functions of the model prior to the model being stored in a structural data base file. (The model can be output in hard-copy form using a Tektronix 4631 that is interfaced to the Tektronix 4014). Creation of the model in the structural data base file (of a CDC 6600) takes the place of creating the model (as was formerly done) via punched cards. The interactive structural modeling method reduces labor and computer modeling and debugging costs by approximately 55%. After the structural data base is created, interactively, the TSO process is continued as it was prior to the introduction of this interactive modeling method.

5. APPLICATIONS OF THE TSO PROCESS

The TSO process, described in the previous sections of this paper, has been used at Honeywell to predict the performance of electro-optical systems that are subjected to thermal/structural environments. Applications of the TSO process are presented in this section for the following sensors: HEAO-B tracker, Sensor A, Sensor B, and ATMOS Fourier transform spectrometer.

5.a. HEAO-B tracker

HEAO-B tracker has a two-mirror aluminum telescope and an ITT image disector tube that are both mounted to the tracker flange that mounts the tracker to an interface bracket of the HEAO-B optical bench. The critical optical system performance requirement was that the operational (in earth orbit) line-of-sight shift (uncalibrated) should not exceed 0.07 arc sec. The primary operational thermal/structural loading comes from thermal soaks and gradients. The operational mechanical stability line-of-sight shift error budget of 0.07 arc sec was subdivided as shown in Table I based on (linearized) optical sensitivities, overall allocation and prior tracker experience. The initial thermal/structural analysis using the TS por-

TABLE I. HEAO-B Tracker Error Budget

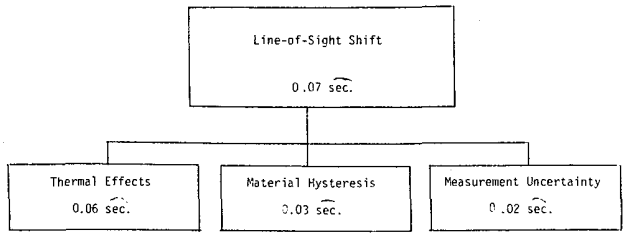

tion of the TSO predicted shifts greater than the total error budget allocation. Reallocation of error budget line items did not meet the overall error budget allocation and so thermal/structural redesign involving MLI, thermal coatings, and telescope housing redesign was performed until the predictions did not exceed error budget line items. The structural deformations were then input with the TSO process that then performed the optical system evaluation that predicted operational line-of-sight shifts of 0.021 arc sec which is less than the thermal/structural induced total allocation of 0.07 arc sec. Table II lists the comparison of the error budget, based on linearized optical sensitivities. Table III lists the comparison of budgets from Table II, the TSO process and empirical data.

5.b. Sensor A

Sensor A is a 150 Hz spinning re-imaging system containing four mirrors in an all-beryllium subsystem that is interfaced to various motor materials and to stainless-steel bearings. The requirements of

TABLE II. HEAO-B LOS Error Budget and Predictions

Error Type	Thermal Effects (uncalibrated) Linearized Sensitivity	Deformation Error Budget	LOS Shift, arc sec
Secondary mirror decenter	-0.50 arc sec/ 151 μin.	5.2 μin.	
Secondary mirror tilt	-0.50 arc sec/ 0.49 arc sec	-0.15 arc sec	
Primary mirror decenter	+0.50 arc sec/ 24.6 μin.	1.6 μin.	
Primary mirror tilt	-0.50 arc sec/ 0.25 arc sec	-0.080 arc sec	
Coil front decenter	-1.0 arc sec/ 58.2 μin.	-1.11 μin.	
Coil at IDT aperture decenter	+1.0 arc sec/ 58.2 μin.	+4.34 μin.	
IDT* aperture decenter	-1.0 arc sec/ 58.2 μin.	-3.13 μin.	
		Total =	0.060 arc sec

(* = Image Dissector Tube)

TABLE III. HEAO-B LOS Error Budget, Predictions, and Empirical Data

Item	LOS Change, Sec
Total LOS error budget	0.07 arc sec
Predicted LOS shift	0.021 arc sec
Empirical LOS shift (Uncalibrated)	0.025 arc sec

the system design addressed in the integrated TSO analyses are listed below:

1. LOS shifts at 26 msec after shock initiation of $\leq$ 0.3 mrad.
2. Room temperature (spinning) blur circle size (95% energy) $\leq$ 2.0 mr.
3. Cryogenic temperature (13 K to 145 K, spinning) blur circle size (95% energy) $\leq$ 1.0 mrad.
4. Minimum structural resonance $\geq$ 400 Hz.

The optical tradeoffs to meet the above requirements are discussed next. The sensor consists of a four-mirror re-imaging design, as shown in Fig. 3. This configuration was necessary in order to

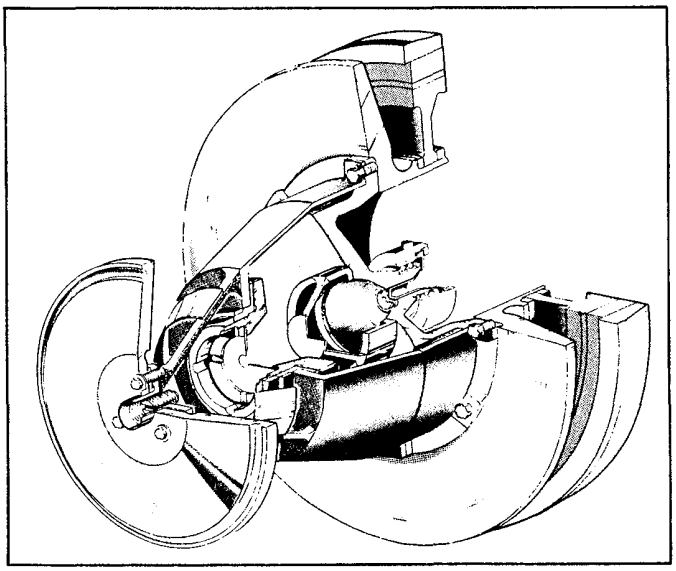

Fig. 3. Sensor A cut-away view.

meet the off-axis rejection requirements. The system aperture stop is at the primary mirror, which is re-imaged at the fourth mirror. The edges of the fourth mirror are painted black to form a Lyot stop. In this way diffracted energy from the primary mirror will be blocked at the Lyot stop. In a similar fashion, "Lyot struts" were placed in front of the detector to block diffracted energy from the struts holding the second mirror. The required image quality was met using two spherical mirrors, one conic, and one general aspheric. In order to assess optical system performance across the range of environmental effects, the following cases were analyzed for each design:

1. Room temperature constant speed spin (no time-varying dynamic inputs);
2. Cooldown with 150 Hz spin and 110G shocks (16 msec trapezoid) to a) 77 K, b) 30 K, c) 13 K.
3. Warm-up from cases 2) at 50 and 120 secs (spin, shocks).

The error budget for thermal/structural effects is shown in Table IV. Initial TSO evaluation of aluminum re-imaging systems

TABLE IV. Sensor A Mechanical Error Budget

	Resolution, MR			
Error Source	Room Temperature Spin		Cryogenic Spin	
1) Nominal design	1.94 MR		0.90 MR	
2) Thermal effects	0.03 MR	1.99 MR	0.06 MR	0.98 MR
3) Spin	0.02 MR		0.02 MR	
4) Tolerances				
a) Optics fab	0.14 MR		0.14 MR	
b) Fab and assembly	0.14 MR		0.14 MR	
5) Post shock	N/A		0.05 MR	
Total Error	2.00 MR		1.00 MR	

Total Error $= \sqrt{[① + ② + ③]^2 + [④a^2 + ④b^2 + ⑤^2]}$

predicted operational resolution of 26 mr which greatly exceeded the thermal/structural allocation of 1.0 mr. Redesign was initiated which included alternatives such as 1) using an all-beryllium optical system and 2) using aluminum mirrors and structure that would be fabricated so that operational loads would deform the mirrors into shapes that would give the required operational resolution. Analyses showed that the aluminum system was not a practical alternative and so the beryllium optical system was chosen. Figure 4 shows predicted resolution, using the TSO process, versus temperature (including warm-up times up to 120 seconds). Table V presents comparisons of requirements and predictions. Empirical data, obtained from spot diagrams presented as Fig. 5, shows that operational resolution (that includes spin and thermal loading effects) of less than the required 1.0 mr was obtained.

5.c. Sensor B

The B sensor is a cryogenic sensor containing an all-beryllium two-mirror system that is interfaced to a scanned focal plane (with several materials) and to a fiber glass thermal isolation system. Mounted to the vacuum housing of the sensor is a laser range finder

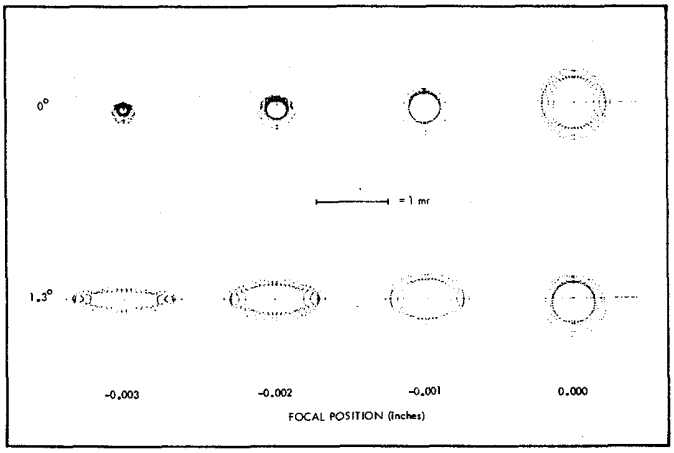

Fig. 5. Sensor A optical spot diagrams.

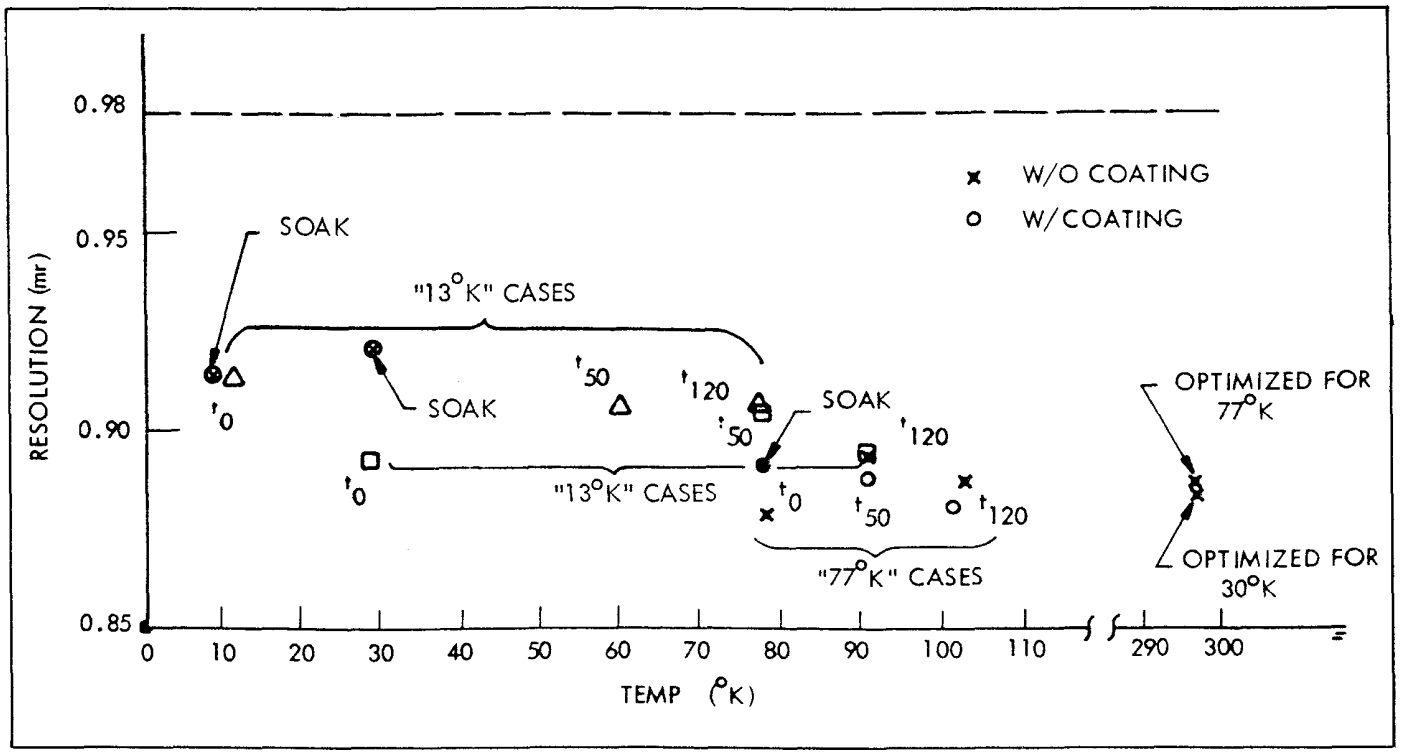

Fig. 4. Sensor A resolution vs "soak temperature."

(LRF) that is boresighted to the sensor boresight. The critical optical system performance operational requirement is maintaining line-of-sight of the sensor versus that of the LRF to 200 μrads, while tracking in the following environments:

1. Temperature changes during mission.
2. Steady state accelerations of 1.25 G's, axial and 0.25 G transverse.
3. Sinusoidal vibration of 0.16 G from 5 to 60 Hz.

A schematic drawing of the sensor is shown in Fig. 6. The sensor

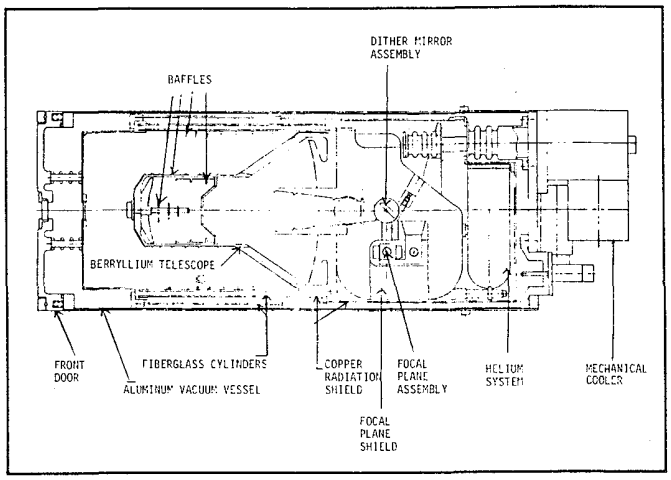

Fig. 6. B sensor schematic.

versus LRF LOS error is listed in Table VI and subdivided among the sensor and the LRF in Tables VII and VIII. Table IX lists the subdivisions of the line-of-sight error budgets, based on optical sensitivities, overall allocation, and previous experiences, for the major items of Tables VII and VIII. Comparisons of the error

TABLE V. Sensor A Design Study

Item	Requirements	Predictions
Weight	0.6 lb	0.593 lb
Angular momentum	2.5 ± 0.5 in.-lbs. at 150 Hz	2.44 in.-lbs. at 150 Hz
Polar/trans. inertia ratio	1.3	1.312
Natural resonance frequency	400 Hz	766.2 Hz
Isoelasticity	±5%	0.5% Radially
Post-shock recovery	≤ 0.3 MR within 10 MS After-shock termination	≤0.024 MR within 10 MS After-shock termination
Safety factor to yield	≥ 1.5	5.1 (Operations) 4.1 (MMIII Envir.)
Blur circle diameter (95%)		
30° - 145° K	≤ 1 MR	≤ 0.935 MR
Ambient	≤ 2 MR	≤ 0.899 MR

TABLE VI. B Mechanical Stability Error Budgets During Processing of LRF and Sensor Data

Error Source	Budget (not to exceed)
Sensor LOS vs alignment mirror	100 μr
LRF XMTR LOS vs sensor LOS	200 μr
LRF XMTR LOS vs XMTR sensor interface	100 μr

TABLE VII. B Mechanical Stability Error Budgets

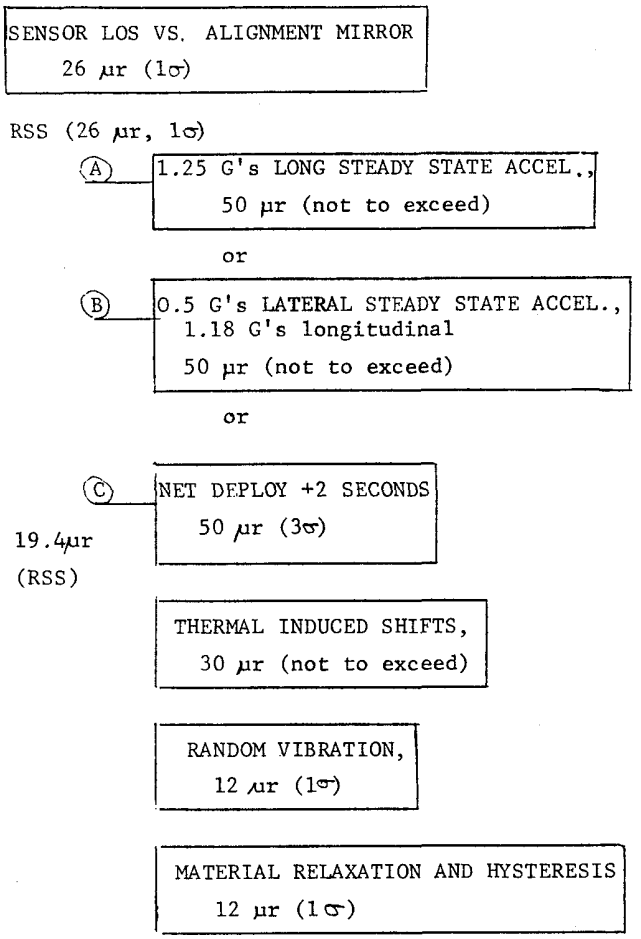

budget line items and predicted thermal/structural effects (empirical data are not yet available) are listed in Table X. During the design cycle, minor redesign of the fiber glass thermal isolation system was necessary to meet some error budget line items.

5.d. ATMOS Fourier transform spectrometer

ATMOS is a Fourier transform spectrometer, to be flown on Space Shuttle Mission 7, to measure minute amounts of molecular constituents in the stratosphere.[6] ATMOS contains an aluminum sun-tracker, aluminum telescope, interferometer (with KBr, A-2 steel, aluminum, CERVIT), laser, and a camera, all mounted to an aluminum-cored construction baseplate which in turn is vibration isolated from a shuttle pallet interface structure.

The interferometer has tilt compensation among the optical elements to that the interferometer is relatively tilt insensitive. Allowable tilts of 1 to 5 arc mins (versus 1 to 2 arc secs for a linear nontilt-compensated system) thus make tilts and linear motion within the interferometer relatively insensitive to thermal/structural induced effects. However the optical requirement for wavefront correction of total wavefront error of $<0.16\lambda$ (peak-to-valley) to produce a fringe contrast of 80% results in sensitivity of optical wavefront to thermal/structural induced effects. The wavefront error requirement leads to the thermal/structural error budgets discussed in this paper. The optical mounts and supporting structures must be designed and fabricated so that errors from fabrication, alignment, and thermal/structural effects will not compromise instrument performance.

The ATMOS interferometer optical schematic is shown in Fig. 7.[7] Energy enters from the fore-optics through an aperture opening

TABLE VIII. B Stability Error Budgets During Processing of LRF and Sensor Data

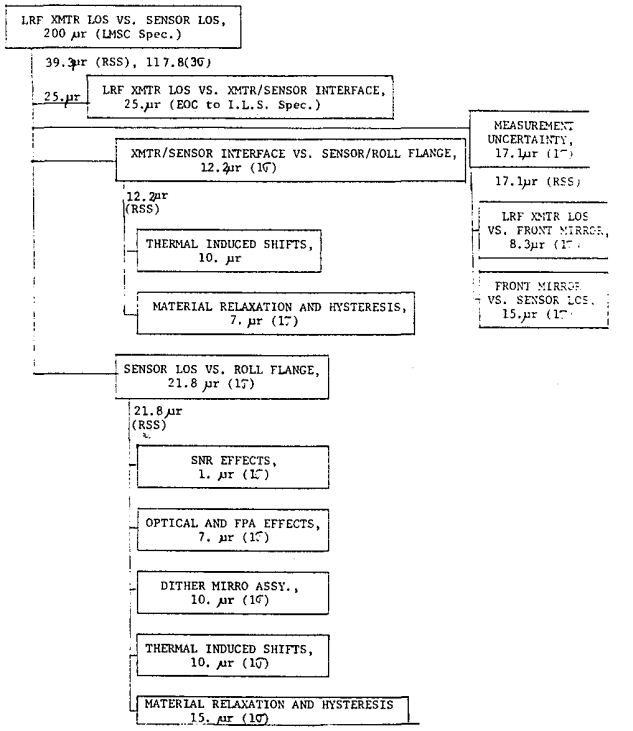

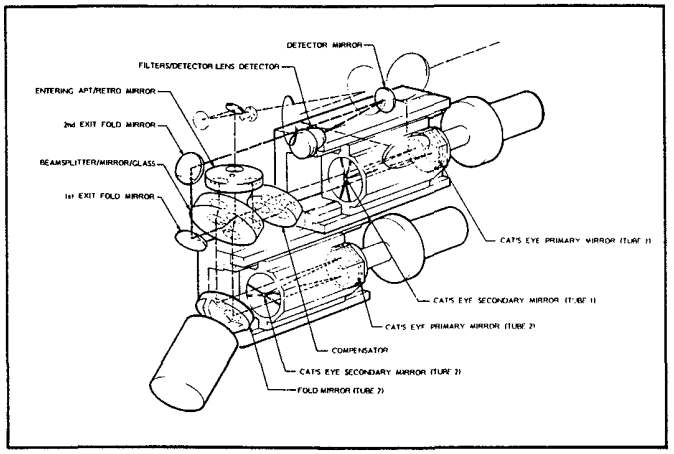

Fig. 7. ATMOS interferometer optics.

in the retroreflector of the interferometer. Part of the entering energy is reflected to the upper cat's eye reflector and part transmitted to the lower cat's eye reflector. In the upper arm, the optical path includes a compensator which equalizes the dispersive material path of the lower arm introduced by the beamsplitter. The combined beams of the two arms are folded by two plane mirrors to a spherical mirror which focuses them at the field image and with a zinc selenide lens images the pupil onto the detectors. The total system error budget is 0.16 λ (P-V at 2 μm) or 0.062 λ (RSS at 2 μm) and budgeting for construction and alignment, and thermal/structural effects is shown in Table XI.[8] As this table shows, the amount allocated in the wavefront error budget for all thermal/structural induced effects is 0.30 λ (RSS at 2 μm). This overall thermal/structural budget is then used subdivided among the components of the interferometer. The mechanical stability error budget for thermal/structural induced effects is listed in Table XII. The total allocated

TABLE IX. B Sensor Stability Error Budgets

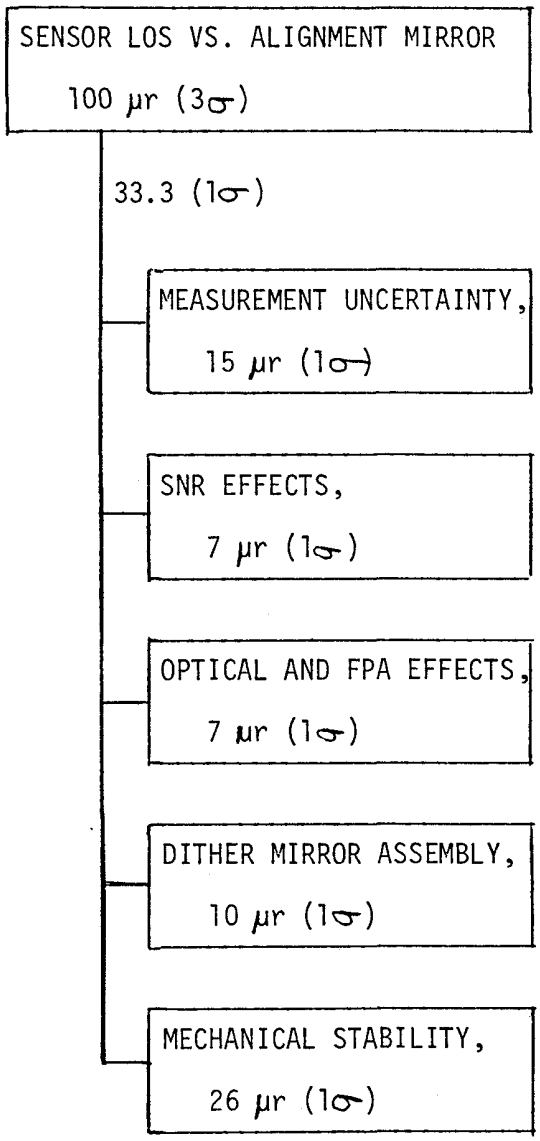

wavefront error of 0.030 λ (RSS at 2 μm) for this error budget matches the allocation (see Table XI) from the overall systems error budget. It is noted that the most significant portion of the error budget is allocated to beamsplitter surface deformations. Comparisons of thermal/structural induced errors (predicted in the next section) are compared subsequently to assess thermal/structural performance versus ATMOS requirements.

Thermal/structural analysis from TS part of TSO showed design problems caused by relative defocus of the two cat's eyes and baseplate thermal gradients. Material changes and component relocation were necessary to meet error budget line items. Results of subsequent TSO analyses are presented as temperatures and comparison of error budget line items and predicted thermal/structural effects in Tables XIII and XIV, respectively. The predicted interferometer operational wavefront change of 0.0061 λ (RMS), at 10 μm, is within the 0.030 λ (RMS), at 10 μm, total error budget allocation.

6. SUMMARY

Methodology to predict thermal/structural performance of electro-optical systems subjected to thermal/mechanical loading that uses

TABLE X. B Sensor Acceleration Deformations

Environment	Component	Deformations	LOS Shift	Total LOS Shift
0.4 g's lateral	Secondary mirror decenter	+14 μin.	+17.6	
1.25 g's longitudinal	Secondary mirror tilt	+27.1 μr	+22.3	
(θ = 20° case)	Primary mirror decenter	+283 μin.	-50.3	Σ = 28.8 μr
	Primary mirror tilt	+27.6 μr	+48.6	
	DMA Decenter	+340 μin.	-12.5	
1.5 g's longitudinal	Secondary mirror decenter	-4 μin.	-1.34	
(θ = 0° case)	Secondary mirror tilt	+1.50 μr	+1.34	
	Primary mirror decenter	+4 μin.	-1.19	Σ = 1.4 μr
	Primary mirror tilt	+1.50 μr	+2.98	
	DMA Decenter	+6.5 μin.	-0.37	

TABLE XI. ATMOS Interferometer RMS Wavefront Error Budget

Parameter	Wavefront Errors (RSS), at 2 μm	
Construction errors	0.055 λ	
Thermal effects	0.024 λ	Mechanical
Nonoperational dynamics, and O-G release	0.016 λ	Disturbance Effects
Operational dynamics	0.006 λ	(0.030 λ)
Total (RSS)	0.062 λ	

TABLE XII. ATMOS Interferometer Wavefront Thermal and Structural Error Budgets

	Component	Error Type	Error Budget Line Item
"Rigid body" motions	Cat's eye P-S(1), (2)	Tilt	5.0 arc min
	Fold mirror	Tilt	3.0 arc min
	Beamsplitter	Tilt	3.0 arc min
	Retro-mirror	Tilt	3.0 arc min
	Compensators	Tilt	5.0 arc min
	Cat's eyes	Relative axial motion	120.0 μin.
Surface deformations (P-V @ 2 μm)*	Fold mirror (2)	Surface figure	0.014 λ
	Beamsplitter (1)	Surface figure	0.047 λ
	Beamsplitter (2)	Surface figure	0.047 λ
	Retro-mirror	Surface figure	0.012 λ
	Retro-mirror (2)	Surface figure	0.012 λ
	Compensators (1)	Surface figure	0.059 λ
	Cat's eyes (1) prim.	Surface figure	0.015 λ
	Cat's eyes (1) sec.	Surface figure	0.012 λ
	Cat's eyes (2) prim.	Surface figure	0.015 λ
	Cat's eyes (2) sec.	Surface figure	0.012 λ
		Totals (P-V) @ 2 μm	0.120 λ
		Totals (RMS) @ 2 μm	0.030 λ

(Note: P-V = Peak-to-valley maximum differences
(n) * = (n), N is number of times energy passes through a surface)

integrated computer-based numerical tools has been presented.

TABLE XIII. ATMOS Temperature Summary (°C)

Component	Cold Case Orbit	Hot Case Orbit
Cold plate temperature	5	45
Baseplate temperature, maximum	-2.8	50.8
Baseplate temperature gradients, maximum		
Across length	0.8	2.2
Across width	0.5	1.0
Through thickness	0.2	0.4
Interferometer temperatures		
Slide 1, maximum	-2.8	49.6
Slide 2, maximum	-2.9	49.2
Slide 1 to 2, max at	0.2	0.52
Beamsplitter	-3.1	49.1
Retro mirror	-3.3	49.4
Compensator	-3.0	49.2
Michelson motor mirror	-3.1	52.6
Laser tube	-3.0	57
Camera	-3.0	51.8
Telescope assembly	-3.5	51.2
Sun sensor	-18.1	54.5

Beamsplitter Thermal Analyses

Thermal Gradient Direction	Thermal Gradient (°C)	
	Solar Flux (0.028 W)	No Solar Flux
Axial	0.063	0.075
Radial	0.075	0.111
Circumferential	0.089	0.002

TABLE XIV. ATMOS Interferometer Wavefront Thermal and Structural Predicted Motions

	Component	Error Type	Predicted Motion
"Rigid body" motions	Cat's eye P-S(1), (2)		0.12 arc min
	Fold mirror	Tilt	0.14 arc min
	Beamsplitter	Tilt	0.13 arc min
	Retro-mirror	Tilt	0.13 arc min
	Compensators	Tilt	0.12 arc min
	Cat's eyes	Relative axial motion	18.2 μin.
Surface deformations (P-V @ 2 μm)*	Fold mirror (2)	Surface figure	0.012 λ
	Beamsplitter (1)	Surface figure	0.025 λ
	Beamsplitter (2)	Surface figure	0.025 λ
	Retro-mirror	Surface figure	0.012 λ
	Retro-mirror (2)	Surface figure	0.012 λ
	Compensators (1)	Surface figure	0.053 λ
	Cat's eyes (1) prim.	Surface figure	0.017 λ
	Cat's eyes (1) sec.	Surface figure	0.012 λ
	Cat's eyes (2) prim.	Surface figure	0.017 λ
	Cat's eyes (2) sec.	Surface figure	0.012 λ
		Totals (P-V) @ 2 μm	0.0244 λ
		Totals (RMS) @ 2 μm	0.0061 λ

(Note: P-V = Peak-to-valley maximum differences
(n) * = (n), N is number of times energy passes through a surface)

This paper has discussed the methods that are used to create mechanical stability error budgets; how the TSO process has automated the interfaces among thermal, structural, and optical programs evaluation of typical systems and comparison of predictions using the TSO process to error budgets and empirical data. Overall cost reductions for the four examples given is 51% versus the manual method formerly used. The overall cost reductions for the TSO process prior to the use of interactive modeling and data

input was previously reported at 47%. Introduction, in 1979, of the interactive modeling and data input (using a Tektronix 4014, digitizing tablet, and UNISTRUC code) has reduced costs further. Honeywell has found that the interactive modeling and data input reduces this part of the TSO process by 55% and reduces the overall TSO process costs by 51%. In addition the automated interfacing of programs has increased accuracy by eliminating inaccuracies from manual data transfer errors and use of spline solutions. This methodology has proven to be a cost-effective means of performing evaluations of electro-optical systems which has also reduced costs and schedules while improving numerical accuracies.

7. REFERENCES

1. Miller, J. M. and Hatch, M. R., Proc. SPIE 121, 146 (1977).
2. Miller, J. M., Proc. SPIE 147, 117 (1978).
3. Key, S. W. and Krieg, R. D., Comparison of Finite Element and Finite Difference Methods, ONR Symposium on Numerical and Computer Methods in Structural Mechanics, Urbana, Illinois, September, 1971.
4. Zienkiewicz, O. C., *The Finite Element Method in Engineering Science,* McGraw-Hill, London (1971).
5. Miller, J. M., Interactive Structural Modelling and Analyses Using UNISTRUC Pre- and Post-Processors and Analysis Programs, presented at 1st Annual Honeywell CAD/CAM Workshop, Minneapolis, Minnesota, November, 1979.
6. Abel, I. R., Reynolds, B. R., Breckinridge, J. B., and Pritchard, J., Proc. SPIE 193, 12 (1979).
7. Honeywell, Inc., ATMOS Final Design and Operations Review, Instrument Optical Design, ENG 014-FDOR, June, 1979, Lexington, Mass.
8. Miller, J. M., Proc. SPIE 216, 186 (1980).